JOC Article

Hydrogen Atom Tunneling in Triplet *o*-Methylbenzocycloalkanones: Effects of Structure on Reaction Geometry and Excited State Configuration

Brent A. Johnson,[†] Mark H. Kleinman,[‡] Nicholas J. Turro,*[,‡] and Miguel A. Garcia-Garibay*[,†]

Department of Chemistry and Biochemistry, University of California, Los Angeles, California 90095, and Department of Chemistry, Columbia University, New York, New York 10027

mgg@chem.ucla.edu

Received October 17, 2001

The rates of phosphorescence decay of 4,7-dimethylindanone (**2**), 6,9-dimethylbenzosuberone (**3**), and several related compounds have been analyzed between 4 and 100 K to determine the contributions of intramolecular hydrogen atom tunneling from the *o*-methyl group to the excited state carbonyl oxygen. Changes in the benzocycloalkanone ring size from five to seven not only affect the geometry at the reaction center, but they also affect the electronic configuration of the triplet excited state in a significant manner. While the triplet state of 5,8-dimethyltetralone (**1**) in nonpolar glasses can be clearly described as having a predominant n,π^* configuration, compounds **2** and **3** have a significantly larger contribution of the less reactive π,π^* state. 4,7-Dimethylindanone (**2**) is stable under cryogenic conditions and in solution at ambient temperature. In contrast, triplet lifetimes and product analysis indicate that 6,9-dimethylbenzosuberone (**3**) reacts by quantum mechanical tunneling at temperatures as low as 4 K. A surprisingly small isotope effect $k_H/k_D \approx 1.1$ between 4 and 50 K increases steadily up to $k_H/k_D \approx 5.1$ at 100 K. This unusual observation is interpreted in terms of a vibrationally activated quantum mechanical tunneling process with hydrogen atom transfer at the lowest temperatures being mediated by zero-point-energy reaction-promoting skeletal motions. Results presented here indicate that the combined effects of increasing π,π^* character and unfavorable reaction geometry contribute to the diminished reactivity of *o*-methyl ketones **2** and **3** as compared to those of tetralone **1**.

Introduction

Reactions that occur by quantum mechanical tunneling have been the subject of numerous theoretical[1−3] and experimental studies, including reactive species in cryogenic rare gas matrices[4] and several biological systems.[5] With a combination of isotope effects, variable-temperature rate measurements, and product detection, it has been shown that adiabatic hydrogen atom transfer (H-transfer) and photoenolization of triplet 5,8-dimethyltetralones (**1a**−**c**) occurs by quantum mechanical tunneling (QMT) at remarkably low reaction temperatures (e.g., 4−100 K).[6−8] While it is known that the rates of QMT depend on the detailed structure of the reaction surface,[1−3] experimental evidence illustrating this dependence is rather limited. To probe the sensitivity of QMT to small changes in the structure of the reactant, we recently analyzed the effects of α-methyl substituents in 5,8-dimethyltetralone (compounds **1a**−**c**).[6a] With a relatively small structural modification away from the reaction center, we intended to probe whether additional vibrational modes and a small steric perturbation in **1b** and **1c** could affect the rates of QMT previously observed with **1a**.[6a,d,7] With triplet decay measurements between 4 and 100 K in methyl cyclohexane (MCH) glasses, we found that one or two α-methyl groups result in insignificant changes in the rate of the QMT reaction.[6a] In this paper,

[†] University of California.
[‡] Columbia University.

(1) Bell, R. P. *The Tunnel Effect in Chemistry*; Chapman and Hall: New York, 1980.
(2) Lee, S.; Hynes, J. T. *J. Chim. Phys. Phys.-Chim. Biol.* **1996**, *1996*, 1783−1807
(3) (a) Truhlar, D. G.; Liu, Y.-P.; Schenter, G. K.; Garret, B. C. *J. Phys. Chem.* **1994**, *98*, 8396−8405. (b) Liu, Y.-P.; Lu, D.; Gonzalez-Lafont, A.; Truhlar, D. G.; Garret, B. C. *J. Am. Chem. Soc.* **1993**, *115*, 7806−7817.
(4) (a) Zuev, P.; Sheridan, R. S. *J. Am. Chem. Soc.* **1994**, *116*, 4123−4124. (b) Chapman, O. L.; Johnson, J. W.; McMahon, R. J.; West, P. R. *J. Am. Chem. Soc.* **1988**, *110*, 501−509. (c) Gol'danskii, V. I.; Benderskii, V. A.; Trakhtenberg, L. I. *Adv. Chem. Phys.* **1993**, *75*, 349.
(5) (a) Kohen, A.; Klinman, J. P. *Chem. Biol.* **1999**, *6*, R191−R198. (b) Kohen, A.; Klinman, J. P. *Acc. Chem. Res.* **1998**, *31*, 397−404. (c) Rucker, J.; Klinman, J. P. *J. Am. Chem. Soc.* **1999**, *121*, 1997−2006.
(6) (a) Johnson, B. A.; Garcia-Garibay, M. A. *J. Am. Chem. Soc.* **1999**, *121*, 8114−8115. (b) Garcia-Garibay, M. A.; Gamarnik, A.; Pang, L.; Jenks, W. S. *J. Am. Chem. Soc.* **1994**, *116*, 12095−12096. (c) Garcia-Garibay, M. A.; Gamarnik, A.; Bise, R.; Jenks, W. S. *J. Am. Chem. Soc.* **1995**, *117*, 10264−10275. (d) Johnson, B.; Gamarnik, A.; Garcia-Garibay, M. A. *J. Phys. Chem.* **1996**, *100*, 4697−4700. (e) Gamarnik, A.; Johnson, B. A.; Garcia-Garibay, M. A. *J. Phys. Chem.*, **1998**, *102*, 5491−5498.
(7) (a) Al-Soufi, W.; Eychmuller, A.; Grellmann, K. H. *J. Phys. Chem.* **1991**, *95*, 2022−2026. (b) Smedarchina, Z.; Enchev, V.; Lavtchieva, L. *J. Phys. Chem.* **1994**, *98*, 4218−29.
(8) A similar hydrogen atom tunneling reaction has been observed in radical ions of analogous compounds: (a) Bednarek, P.; Zhu, Z.; Bally, T.; Filipiak, T.; Marcinek, A.; Gebicki, J. *J. Am. Chem. Soc.* **2001**, *123*, 2377−2387. (b) Marcinek, A.; Adamus, J.; Huben, K.; Gebicki, J.; Bartczak, T. J.; Bednarek, P.; Bally, T. *J. Am. Chem. Soc.* **2000**, *122*, 437−443.

10.1021/jo016210r CCC: $22.00
Published on Web 09/07/2002

SCHEME 1

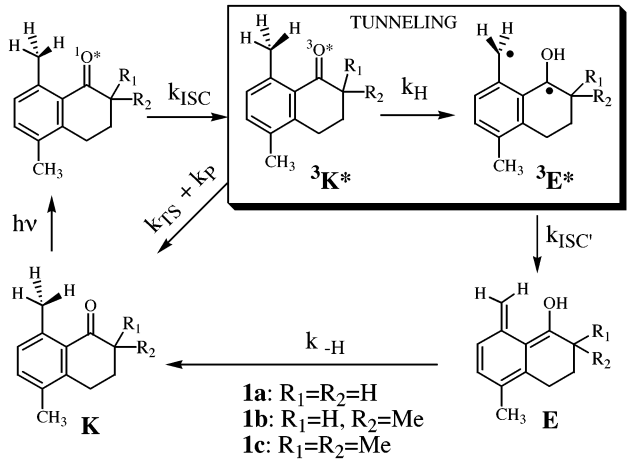

SCHEME 2

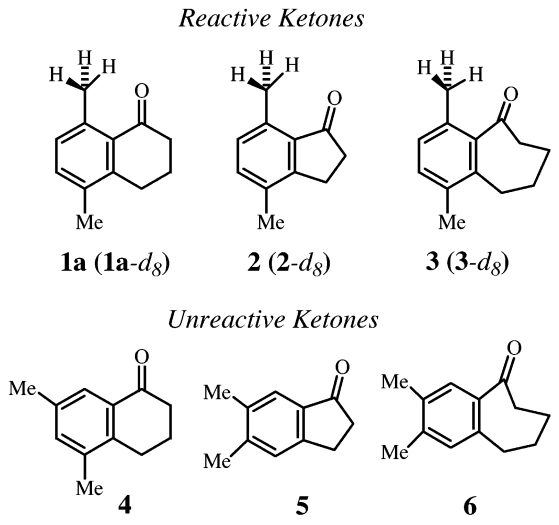

we explore how other structural and electronic factors may affect the rate of the H-transfer reaction. We analyzed the low-temperature reactivity of 4,7-dimethylindanone (**2**), 6,9-dimethylbenzosuberone (**3**), and their deuterated analogues **2**-d_8 and **3**-d_8 (Scheme 2). At first sight, the nearly identical 2,3,6-trialkyl substitution pattern on the basic aryl ketone chromophore in compounds **1**, **2**, and **3** suggests that the rates of H-transfer may reflect differences in the distances and orientation between the atoms involved in the reaction. However, small changes in the dihedral angle between the planes of the carbonyl and phenyl groups are also known to affect the electronic properties of the triplet excited state of the aryl ketone chromophore.[9] It is well-known that energetically close states with different electronic configurations may mix upon a proper perturbation to give hybrid states possessing photophysical and photochemical properties that lie between those of the original states.[10−12] The results of measurements carried out between 20 and 100 K reported here did reveal some of these complexities. While the triplet state of 5,8-dimethyltetralone (**1**) in nonpolar media can be described as possessing a predominant n,π^* character,[6,7] the triplet state configurations of **2** and **3** have a significantly larger contribution of the less reactive π,π^* configuration.[13] Remarkably, despite having an abstractable hydrogen within relatively close proximity of the carbonyl oxygen, 4,7-dimethylindanones **2** and **2**-d_8 were photostable at cryogenic temperatures in glassy matrices and in fluid solution at ambient temperatures. With reactivity that falls between those of **1a** and **2**, 6,9-dimethylbenzosuberones **3** and **3**-d_8 undergo excited state H- and D-atom tunneling with relatively slow rates. A small and relatively constant isotope effect value of $k_H/k_D = 1.1$ between 20 and 50 K increases up to a value of $k_H/k_D = 5.1$ as the temperature is increased above 50 K. This unusual temperature dependence of the isotope effect has been interpreted in terms of a vibrationally assisted tunneling mechanism.[14] The kinetic results from these experiments were analyzed in terms of the ground-state structures determined by X-ray diffraction and molecular mechanics calculations. We conclude that the combined effect of a π,π^* triplet character and unfavorable reaction geometry contribute to the reduced reactivity of compounds **2** and **3**.

Experimental Section

Compounds **2**,[15] **3**,[15b] **5**,[16] and **6**[17] were prepared with commercial (Aldrich Chemical Co) *p*-xylene and *p*-xylene-d_{10} (**2**-d_8, **3**-d_8, **5**-d_8, and **6**-d_8) by reported procedures and were fully characterized.[14b] X-ray diffraction data for compounds **2** and **3** were acquired at 296 and 150 K, respectively. Crystallographic structure solution and refinement are included in the Supporting Information. All samples were freshly distilled, sublimed, and/or purified by chromatography immediately prior to use. Solvents used were of the highest purity available. Ketones were diluted to concentrations between 3.0×10^{-5} and 10×10^{-5} M in MCH or EtOH. Low concentrations were used to avoid aggregation or microcrystallization. Phosphorescence measurements were taken by front face detection in a SPEX-Fluorolog spectrometer equipped with a 1943D phosphorimeter and an R 928 PMT detector. Measurements were taken with an initial acquisition delay of 0.04 ms to avoid scattering from the 10-μs lamp pulse. Acquisition windows and delay increments of the same length were optimized to obtain between 100 and 300 data points per decay. Variable-temperature measurements were obtained in a 1 mm path length quartz cuvette immersed in an Oxford Optistat Bath liquid helium cryostat. Temperature control was done automatically by an Oxford ITC 601 temperature controller.

Laser flash photolysis experiments employed pulses (XeCl, 308 nm, <30 mJ/pulse, pulse duration of 5−10 ns) from a

(9) Turro, N. J.; Gould, I. R.; Liu, J.; Jenks, W. S.; Staab, H.; Alt, R. *J. Am. Chem. Soc.* **1989**, *111*, 6378−83.
(10) Turro, N. J. *Modern Molecular Photochemistry*; Benjamin Cummings Publishing Co.: Menlo Park, CA, 1978.
(11) Berger, M.; McAlpine, E.; Steel, C. *J. Am. Chem. Soc.* **1978**, *100*, 5147−51.
(12) Wagner, P. J.; Kemppainen, A. E.; Schott, H. N. *J. Am. Chem. Soc.* **1973**, *95*, 5604−5614.
(13) (a) Yang, N. C.; McClure, D. S.; Murov, S. L.; Houser, J. J.; Dusenbury, R. *J. Am. Chem. Soc.* **1967**, *89*, 5466−5468. (b) Case, W. A. *J. Chem. Phys.* **1970**, *52*, 2175−2191. (c) Case, W. A.; Kearns, D. R. *J. Chem. Phys.* **1970**, *52*, 2175−2191.
(14) (a) Johnson, B. A.; Hu, Y.; Houk, K. N.; Garcia-Garibay, M. A. *J. Am. Chem. Soc.* **2001**, *123*, 6941−6942. (b) Johnson, B. A. Ph.D. Thesis, University of California, Los Angeles, CA, 1999. (c) A detailed derivation of eq 3 is also available in the Supporting Information section of ref 6a.
(15) (a) Khalaf, A. A.; Abdel-Wahab, A.-M. A.; El-Khawaga, A. M.; El-Zohry, M. F. *Bull. Soc. Chim. Fr.* **1984**, *1984*, 285−291. (b) Bergmark, W. R.; Barnes, C.; Clark, J.; Paparian, S.; Marynowski, S. *J. Org. Chem.* **1985**, *50*, 5612−5615.
(16) Fisnerova, L.; Kakac, B.; Nemecek, O.; Simek, A.; Vejdelek, Z. J. *Collect. Czech. Chem. Commun.* **1967**, *32*, 4082−4098.
(17) Brugidou, J.; Christol, H.; Sachetto, J. P. *Bull. Soc. Chim. Fr.* **1967**, *7*, 2579−2584.

Lambda Physik 50 excimer laser. The system and data acquisition process has been described elsewhere.[18] For all experiments the solutions were deoxygenated by bubbling argon through the solution for at least 20 min. Spectra and kinetics were taken with use of static Suprasil 1 cm × 1 cm quartz cells. All data were obtained from samples at room temperature and exposed to fewer than 50 laser pulses.

Results and Discussion

Determination of Reaction Rates from Phosphorescence Measurements. The reaction mechanism in Scheme 1 is well established.[19−21] High yields of the triplet ketone ^{3}**K*** are formed by a rapid intersystem crossing after the initial excitation of the aryl ketone chromophore. An adiabatic hydrogen transfer dominates the triplet decay at ambient temperatures to give a triplet enol ^{3}**E***. Within a few microseconds, the triplet enol decays to the ground state **E** and the latter reverts to the starting ketone by a proton transfer to complete a fully reversible cycle.

To compare the effect of structure and ring size on the rates of quantum mechanical tunneling, the reaction kinetics must be analyzed at cryogenic temperatures. By slowing the rate of a thermally activated reaction to the limit where tunneling is dominant, kinetic data may be obtained by simple emission techniques. To accomplish that, we consider that the rates of triplet decay (k_{dec}) are the sum of thermal and radiative rates ($k_{TS} + k_P$, see Scheme 1) plus the rate of the hydrogen transfer reaction (k_H, eq 1).

$$k_{dec} = k_{TS} + k_P + k_H \qquad (1)$$

While emission techniques are ideally suited for the measurement of radiative transients in crystalline and amorphous solids, there are some limitations to consider. To obtain the value of k_H, we must assume that the first two rates ($k_{TS} + k_P$) may be obtained from model compounds with similar chromophores but with no excited state reaction possible. To determine these values for compounds **2** and **3**, we have analyzed the photophysical properties of 2,3-dimethylindanone (**5**) and 2,3-dimethylbenzosuberone (**6**, Scheme 2). A concern with this approach is that differences in the position of the methyl groups may give different values of k_{TS} and k_P for test and model compounds. However, compound **4** was recently used as a photophysical model for compound **1a** and the rate constants obtained with eq 2 were consistent with those obtained by flash photolysis methods.[6d] Furthermore, differences in the values of k_{TS} and k_P between sample and model compounds will give rise to systematic errors in the calculated rate constants for k_H but will not affect conclusions drawn from the temperature dependence of the decay observed in the reactive compounds.

Another complication of the emission method is that triplet decays in glassy matrices at low temperatures are highly heterogeneous, so that nonexponential analysis is required. The nonexponentiality of the triplet decay may be due to conformational and/or environmental heterogeneity and is a general feature of amorphous matrices. Given the relatively modest signal-to-noise ratio and the limited amount of data available in a point-by-point decay, we decided to fit the decay data to double exponential functions (eq 2) rather than to use more complex kinetic treatments. Although deviations were generally observed at long decay times, the two components represented the decay in a satisfactory manner with small deviations occurring at the longest decay times. Rather than emphasizing the possible meaning of the two components (which may be an approximation for a complex distribution of lifetimes), we calculated average decay rates, k_{av}, as indicated in eq 3.[14b,c] Equation 3 derives from the integrated contribution from each component ($A_i = I_i/k_i$), with I_i and k_i representing the corresponding preexponentials and rate constants.[14b,c] Average decay rates calculated in this manner for **2** and **3** at 77 K are summarized in Table 1.

TABLE 1. Fit Parameters of Phosphorescence Decay Data in MCH at 77 K with Eq 2

ketone[a]	I_1	I_2	k_1 (s^{-1})	k_2 (s^{-1})	k_{av} (s^{-1})
1-d_8	7609	4060	5580	1810	2431
4	7428	2375	120	27	41
2	8068	2157	12.1	43.7	13.1
2-d_8	7220	2693	7.35	26.8	8.1
5	5558	4996	10.7	19.4	13.1
3	4634	5145	523	103	117
3-d_8	7392	2943	131	78.9	103.7
6	4690	5023	67	28.7	34

[a] Data for compounds **1**-d_8 and **4** are taken from ref 6d.

$$I = I_1 e^{-k_1 t} + I_2 e^{-k_2 t} \qquad (2)$$

$$k_{av} = (I_1/k_1 + I_2/k_2)/(I_1/k_1^2 + I_2/k_2^2) \qquad (3)$$

Phosphorescence Spectra and Decay Data. Phosphorescence measurements in *o*-methyl ketones such as **1a**, **2**, and **3** provide a detailed picture of the electronic configuration and kinetics of their triplet excited states. Aryl ketones with n,π^* electronic configuration have short-lived triplets (ca. $\tau_T \approx 3$ ms) with a vibrational resolution of ca. 1700 cm^{-1} characteristic of vibronic coupling with the carbonyl stretching mode.[10] Ketones with π,π^* configuration have significantly longer lifetimes (i.e., 100 ms), and broad emission spectra due to overlapping vibronic coupling with several aromatic ring vibrational modes.[10] State mixing gives ketones with excited states properties that are somewhere in between.[9−12]

The results of phosphorescence measurements with 4,7-dimethylindanone (**2**), d_8-4,7-dimethylindanone (and **2**-d_8), and 2,3-dimethylindanone (**5**) in MCH suggest a triplet state with a predominant π,π^* electronic configuration. Figure 1 shows the phosphorescence emission of the three compounds at 77 K. The three spectra are very similar to each other although those of **2** and **2**-d_8 are red shifted by about 5 nm with respect to the spectrum of **5**. All three indanones have spectra that are significantly broader than those of the six-membered-ring tetralones reported previously, indicating significantly greater π,π^* character. The emission decays of **2** and **2**-d_8 were fit to double exponential functions and the values

(18) McGarry, P. F.; Cheh, J.; Ruiz-Silva, B.; Hu, S.; Wang, J.; Nakanishi, K.; Turro, N. J. *J. Phys. Chem.* **1996**, *100*, 646−654.
(19) Wagner, P. J.; Chen, C.-P. *J. Am. Chem. Soc.* **1976**, *98*, 239−241.
(20) Akiyama, K.; Ikegami, Y.; Tero-Kubota, S. *J. Am. Chem. Soc.* **1987**, *109*, 2538−2539.
(21) Das, P. K.; Encinas, M. V.; Small, R. D., Jr.; Scaiano, J. C. *J. Am. Chem. Soc.* **1979**, *101*, 6965−6970.

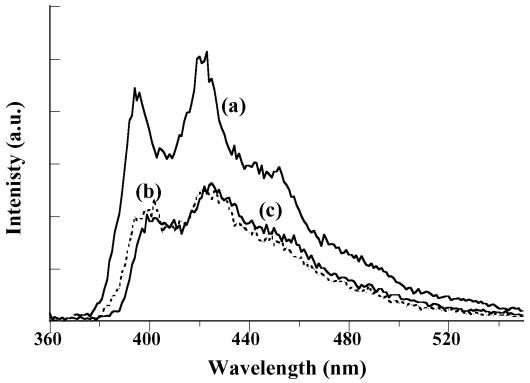

FIGURE 1. Phosphorescence spectra of (a) 5,6-dimethylindanone (**5**), (b, dashed line) 4,7-dimethylindanone (**2**), and (c) d_8-4,7-dimethylindanone (**2**-d_8) in MCH glasses at 77 K.

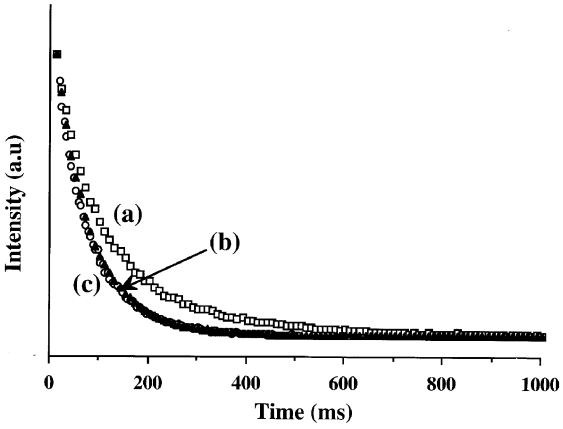

FIGURE 2. Phosphorescence decay of (a) d_8-4,7-dimethylindanone (**2**-d_8), (b) 4,7-dimethylindanone (**2**), and (c) 5,6-dimethylindanone (**5**) in MCH glasses at 77 K.

obtained from the fit are given in Table 1 along with the average decay rates calculated for each compound. As illustrated in Figure 2, the phosphorescence decay of indanone **5** and the *o*-methyl-substituted compound **2** are almost identical, with average rates of 13.1 s^{-1}. The decay rate of the deuterated compound **2**-d_8 is slightly slower with an average rate of 8.1 s^{-1}. The average decay rates of these ketones are a factor of 20−40 slower than those of compounds with n,π^* excited states (e.g., for benzophenone, k_{decay} = 370 s^{-1}). The fact that the average decay rate of **5** is about the same as that of **2** and faster than the average decay rate of **2**-d_8 suggests that both **2** and **2**-d_8 are unreactive. This conclusion was also supported by the lack of photoproduct formation under intense illumination at low temperatures (vide infra).

Phosphorescence measurements with 6,9-dimethylbenzosuberone (**3**), d_8-6,9-dimethylbenzosuberone (**3**-d_8), and 2,3-dimethylbenzosuberone (**6**) in MCH were consistent with excited states of mixed electronic configurations. Figure 3 shows the phosphorescence spectra of these compounds at 77 K in MCH. The emission of **3** and **3**-d_8 is blue shifted by 5 nm relative to that of compound **6**. Compared to the indanones, the spectra of the benzosuberones have greater resolution of the C=O vibrational progression, suggesting a larger n,π^* character. The decay data were fit to a double exponential and the two components were used to calculate the average decay

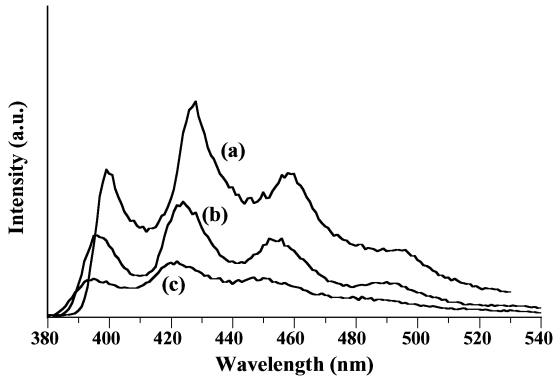

FIGURE 3. Phosphorescence spectra of (a) 7,8-dimethylbenzosuberone (**6**), (b) d_8-6,9-dimethylbenzosuberone (**3**-d_8), and (c) 6,9-dimethylbenzosuberone (**3**) in MCH glasses at 77 K.

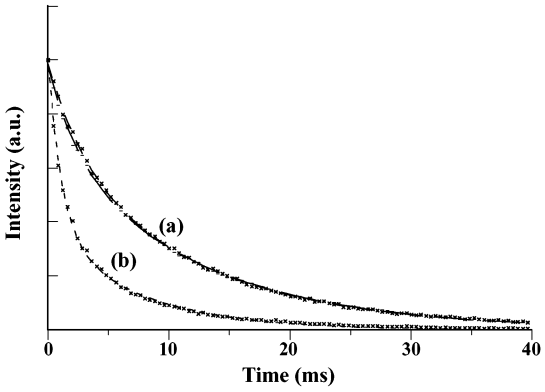

FIGURE 4. Triplet decay of 6,9-dimethylbenzosuberone (**3**) at (a) 20 and 40 K (superimposed) and (b) at 90 K in MCH glass.

rates. As expected for compounds with reactive pathways, the decay rates of **3**-d_8 and **3** were three to four times greater than the decay of compound **6**.

Temperature Dependence of Triplet Decay. We have shown that aromatic ketones without favorable intramolecular reaction pathways present no changes in triplet decay as a function of temperature between 20 and 100 K. This observation indicates that neither radiative decay (k_P) nor intersystem crossing to the ground state (k_{TS}) have a significant temperature dependence. However, a decrease in the excited-state lifetimes in those compounds is observed when the glassy matrix softens above 100 K, suggesting that deactivation occurs by diffusion-mediated quenching processes, including reactions with the hydrocarbon matrix. In contrast, we have found that the temperature dependence of aromatic ketones with favorable intramolecular H-transfer reactions is biphasic: decay rates below 30−40 K are constant, and then they augment considerably as the temperature increases. As indicated by eq 1, the triplet decay rates in reactive compounds include contributions from photophysical processes ($k_P + k_{TS}$) and from the hydrogen transfer reaction (k_H). However, as indicated in eq 4, the rate of hydrogen transfer contains contributions from reactions that occur by quantum mechanic tunneling (k_{QMT}), and reactions that occur by a thermally activated process (k_T). Reactions that occur below 30−40 K proceed by quantum mechanical tunneling along the zero-point-energy surface and have no temperature dependence.

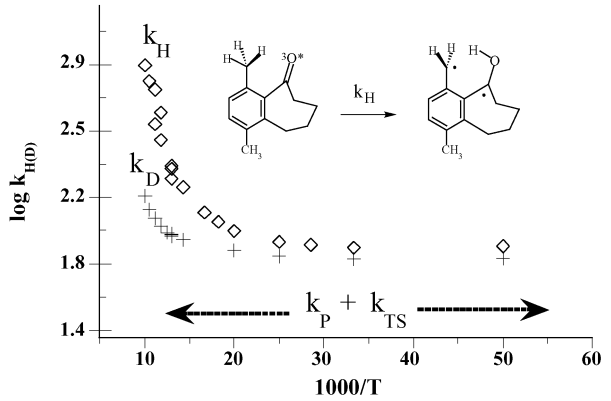

FIGURE 5. Arrhenius plot of the calculated hydrogen and deuterium transfer rates of compounds **3** and **3**-d_8 in MCH glass between 100 and 20 K.

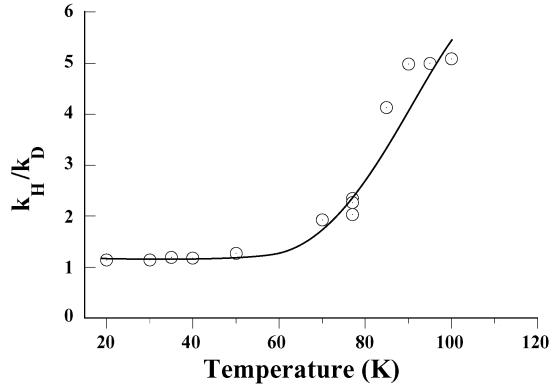

FIGURE 6. Isotope effects calculated from the hydrogen and deuterium transfer rates of compounds **3** and **3**-d_8 in MCH glass between 4 and 100 K.

Product formation at these temperatures proceeds with the lowest possible kinetic energy, with probabilities that are determined by uncertainties in the position of the tunneling particle as given by the zero-point-energy vibrational wave function and its permeability through the barrier. The activation of reaction-promoting modes above 30−40 K allows for some molecules to pass over the barrier with rates k_T that can compete with the rate of triplet decay by photophysical and tunneling processes. An increase in the rates of reaction is also expected at higher temperatures from tunneling processes along higher vibrational surfaces.

$$k_H = k_{QMT} + k_T \qquad (4)$$

Dimethylindanones **2**, **2**-d_8, and **5** showed no changes in decay rates between 20 and 100 K in MCH. This observation, combined with the fact that the decay rates of **2**, **2**-d_8, and **5** are very similar to each other, suggests that neither **2** nor **2**-d_8 is reactive below 100 K. Accordingly, flash photolysis experiments at ambient temperature with **2** resulted in detection of a long-lived triplet excited state, but we were unable to detect the formation of a photoproduct.

A change in ring size from five to seven gave rise to remarkable kinetic differences. Variable-temperature measurements in MCH between 20 and 100 K with **3** and **3**-d_8 showed the biphasic behavior that characterizes the phosphorescence decays of reactive compounds (Figures 4 and 5). We established that reaction rates of **3** remain the same between 20 and 40 K ($k_H = 0.8 \times 10^2$ s^{-1}) and increase by a factor of 5.6 when the temperature is increased to 90 K ($k_H = 4.5 \times 10^2$ s^{-1}). Similarly, the reaction rate of **3**-d_8 shows no significant changes between 20 and 50 K and increases by a factor of 2.5 from 50 ($k_D = 0.6 \times 10^2$ s^{-1}) to 90 K ($k_D = 1.5 \times 10^2$ s^{-1}). To calculate the hydrogen transfer rates for compounds **3** and **3**-d_8 we had determined the values of $k_P + k_{TS}$ from the model dimethylbenzosuberones **6** and **7**. The d_8-6,8-dimethyl derivative **7** became available by an unexpected rearrangement in a Friedel−Crafts reaction that was carried out to prepare a given lot of **3**-d_8. As expected, neither **6** nor **7** displayed changes in triplet decay between 100 and 20 K, and their average decay rates were very similar to each other: 34 and 30 s^{-1}, respectively.

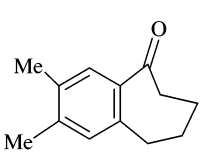

6

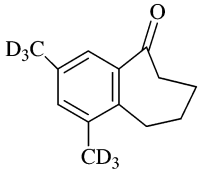

7

The similar decay rates of compounds **6** and **7** support our assumption that the photophysical decay rates of structurally similar chromophores should be essentially the same and downplay the possibility of major photophysical changes due to the different positions of their methyl groups. The Arrhenius plot constructed with data from compounds **3** and **3**-d_8 in Figure 5 illustrates the difference between k_H and k_D with respect to $k_P + k_{TS}$. The temperature dependence of the reaction rate constants of dibenzosuberones **3** and **3**-d_8 is generally consistent with results previously obtained with the tetralones **1a**-d_8 to **1c**-d_8. However, quantum mechanical tunneling from zero-point-energy levels in the case of **3** and **3**-d_8 (ca. 70−100 s^{-1}) was significantly slower than those of **1a**-d_8 to **1c**-d_8 (ca. 10^3 s^{-1}). The most striking and unexpected result in the case of **3** and **3**-d_8 comes from the magnitude of the isotope effect and from its temperature dependence (Figure 6).

Isotope Effects in 6,9-Dimethylbenzosuberone. Because of a very fast hydrogen transfer reaction, we were unable to detect any emission from nondeuterated compounds in previous studies with tetralones **1a**−**c**. In contrast, the emission yields and lifetimes of benzosuberones **3** and **3**-d_8 are remarkably similar. The temperature dependence of the isotope effect calculated from the rate data is shown in Figure 6. The figure illustrates a constant isotope effect $k_H/k_D = 1.13$ between 4 and 50 K and a surprising increase of $k_H/k_D = 5.1$ up to about 100 K when the glassy matrix began to soften.

The results in Figure 6 were unexpected and cannot be explained by a mechanism where the event of hydrogen transfer is the rate-limiting step. A rate-limiting, primary kinetic isotope effect originating from differences in zero-point energies between the two isotopomers is expected to increase exponentially with decreasing temperatures. Furthermore, the magnitude of a primary kinetic isotope effect near 20 K would be too large to be

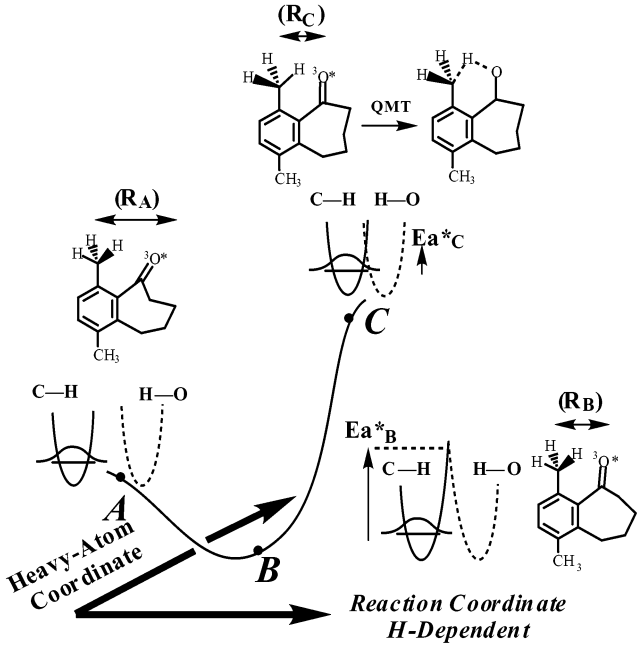

FIGURE 7. Schematic representation of the mechanism for a vibrationally assisted tunneling reaction. See text for details.

measurable with the dynamic range given by emission techniques.[6c,22] Although the temperature invariance of the reaction rate and isotope effect below ca. 50 K requires a tunneling mechanism, the k_H/k_D value for reactions with a rate-limiting H-tunneling reaction from zero-point-energy levels has been calculated to be ca. 10^3.[7]

To explain the results in Figure 6 we propose that H(D)-atom transfer is not the rate-limiting step in the decay of ^{3}**3***. The results require a mechanism where tunneling is mediated by hydrogen isotope-independent motions that occur from zero-point-energy levels, and which become non-rate-limiting when upper vibrational states are populated. A model illustrating this proposal is shown in Figure 7. The reaction coordinate is represented by two potentials corresponding to the C−H bond in the reactant (solid line) and the H−O bond in the product (dashed line). The expectation value of the vibrational wave function describing the position of the hydrogen is shown to extend beyond the classical potential of the reactant. It is known that quantum mechancal tunneling depends on the permeability of the reactant wave function through the barrier that separates it from the final product. The tunneling permeability is inversely proportional to the mass of the tunneling particle (H vs D), and to the height (**Ea***) and the width (**R**) of the activation barrier. As shown in the figure, the transition state energy **Ea*** and the distance **R** between the two curves representing the reactant and the product depend on the structure of the molecule. We suggest that the equilibrium structure of **3**, represented in Figure 7 by point **B**, has a high and wide barrier, which is not conducive to quantum mechanical tunneling. However, an orthogonal heavy-atom coordinate representing skeletal motions can modulate the distance between the two potential wells so that the height (**Ea*$_C$**) and width (**R$_C$**) of the barrier decrease and tunneling becomes possible near point **C**.

SCHEME 3

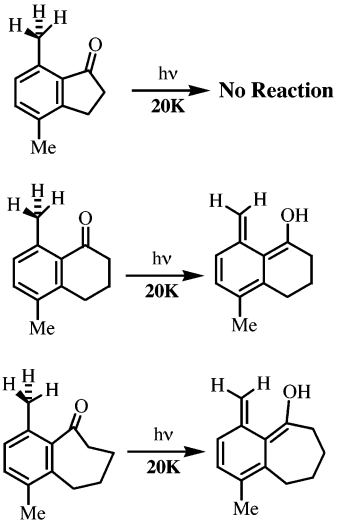

The small isotope effect, its temperature invariance below 50 K, and the increase observed in the k_H/k_D value at higher temperatures can be fit by the proposed model. A simple kinetic expression that reflects this is given by eq 5. The rate constant at the lowest temperatures is given by a heavy-atom-limited, zero-point-energy tunneling rate k_{ZPE}. At higher temperatures, the rate of tunneling increases with a term $k_{VA}\exp(-E_P/RT)$, as higher vibrational states of the promoting mode are populated. The temperature dependence of the rate constant and isotope effect can be fit assuming a reaction-promoting mode with energy E_P = 250 cal/mol, or 87 cm^{-1}. A vibrational analysis of triplet **3** and its transition

$$k_{H(D)} = k_{ZPE} + k_{VA}\exp(-250/RT) \qquad (5)$$

state obtained by density functional methods (B3LYP/6-31G*) shows that hydrogen transfer from carbon to oxygen may be facilitated by modes involving oscillation of the methyl group, at 154 cm^{-1}, and coplanarization of the carbonyl and phenyl groups, at 65.8 cm^{-1}. These occur at 106.7 and 62.7 cm^{-1}, respectively, for the deuterated compound.[14a] It may be noted that tunneling may occur along several vibrational dimensions including heavy atoms and the hydrogen being transferred. Further analysis of this process is in progress and will be published elsewhere.

Enol Accumulation. The accumulation of photoenols by high-intensity irradiation at low temperatures gives a qualitative confirmation of the quantum mechanical tunneling reaction. Since enols revert rapidly to the starting ketone by reverse hydrogen transfer in nonpolar media, enol accumulation must be carried out in polar solvents where their lifetimes are known to be significantly longer.[23] Although polar media changes the configuration of the ketone chromophore and reduces the efficiency of hydrogen transfer, we have shown that

(22) The analytical limits of the emission method are given by the low emission yields when the rate of reaction is too large (ca.. 10^6 s^{-1}), and by the small changes in lifetimes and intensities when the reaction is too slow (ca. 10 s^{-1}).

(23) Baron, U.; Bartlet, G.; Eychmuller, A.; Grellman, K.-H.; Schmitt, U.; Tauer, E.; Weller, H. *J. Photochem.* **1985**, *28*, 187−195.

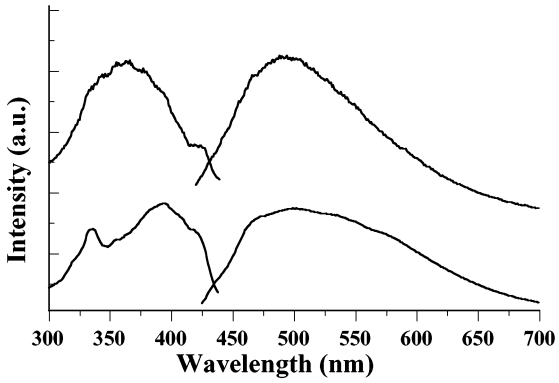

FIGURE 8. Fluorescence excitation (left) and emission (right) of the photoenols obtained by irradiation of **3** (bottom) and **3**-d_8 (top) at 20 K in ethanol.

photoenols can be detected by their yellow color and by their intense fluorescence emission at about 500 nm (Figure 8).[24,25]

Irradiation of 4,7-dimethylindanones **2** and **2**-d_8 at 20 and 77 K failed to produce any detectable photoenol (Scheme 3). We interpret the lack of product formation, and flash photolysis results mentioned below, as indicative of nonexistent (or extremely inefficient) tunneling reaction. Although a fast ketonization would also be possible, there is strong experimental evidence that ketonization rates are slow in polar solvents. In contrast to the indanones, the yellow color of the enol from 6,9-dimethylbenzosuberone (**3**) and its deuterated analogue were accumulated by photolysis in EtOH at 20−25 K for 60 min. Figure 8 illustrates the fluorescence excitation and emission of the enols from ketones **3** and **3**-d_8, which are consistent with each other and with those of other well-documented *o*-quinodimethanes, including the photoenol obtained from **1a** that was reported previously.[6d]

Flash Photolysis Measurements. The spectra and kinetics of reactive intermediates produced by 308-nm excitation of **1a**−**4** were observed by using laser flash photolysis at room temperature. In a fashion similar to that of the unsubstituted tetralone, photolysis of **4** in methylcylohexane yielded transients with $\lambda_{max} < 310$ nm and $\lambda_{max} = 415$ nm with lifetimes of 0.5 and 20 μs, respectively. On the basis of the photochemistry of acetophenone,[26] these transients were assigned to be the triplet excited state (shorter lived) and the ketyl radical (longer lived), which is formed from a hydrogen atom abstraction from the solvent. Only the triplet species with a lifetime of 3 μs is detected in benzene. Experiments conducted with dimethylindanone (**2**) featured the same spectra and kinetic characteristic of **4**. This demonstrates that indanone **2** is unreactive toward intramolecular enol formation both under cryogenic conditions and at ambient temperatures. In the case of **1a**, the transient spectrum shows a strong signal with $\lambda_{max} = 350$ nm. In this case, there is a single lifetime of 150 ns when monitored at 430 nm. Dimethylbenzosuberone (**3**) had the same spectral characteristics as **1a**, except that the transient decayed over 70 ns (observed at 400 nm). The transient was monitored at these wavelengths because the enol is expected to absorb in this region.[7] This transient is attributed to the enol and is presumably formed within the laser pulse (10 ns).

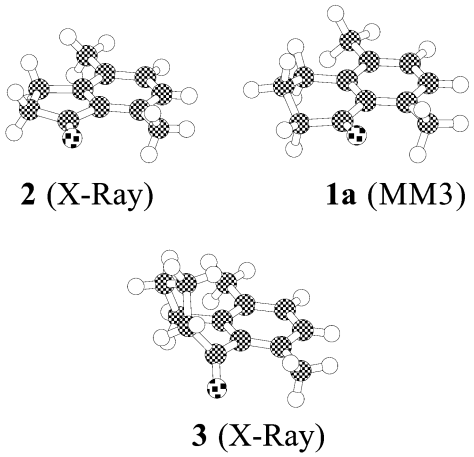

FIGURE 9. Comparison of the X-ray structures of dimethylindanone (**2**) and dimethylbenzosuberone (**3**) (one of two similar structures in the crystal) with the MM3 structure of dimethyltetralone (**1a**).

X-ray Structures and Molecular Mechanics Calculations. To rationalize the differences in quantum mechanical tunneling between ketones **1a**, **2**, and **3** we analyzed their molecular structures by X-ray diffraction and molecular mechanics calculations with the MM3 force field using the program MacroModel (Figure 9). Ketones **2** and **3** were crystallized by slow evaporation from saturated hexane solutions. Unfortunately, we were not able to obtain suitable crystals of dimethyltetralone (**1a**) after repeated attempts. We noticed that the melting point of dimethylindanone (**2**) (35 °C) is remarkably close to that of dimethyltetralone (**1a**) (32 °C),[27] suggesting that they may have similar packing arrangements. The melting point of dimethylbenzosuberone (**3**) is 75−76 °C. It is indicative of a different arrangement and intermolecular forces. Crystallographic data and refinement parameters for compounds **2** and **3** are included in the Supporting Information.

Dimethylindanone (**2**) crystallized in the triclinic space group $P\bar{1}$ and dimethylbenzosuberone (**3**) in the monoclinic space group $P2_1/c$. The structure of 4,7-dimethylindanone (**2**) is nearly flat, with the planes of the aromatic and carbonyl groups making a dihedral angle of only 3.0° (Figure 9). The X-ray structure of dimethylbenzosuberone (**3**) revealed a pseudoboat conformation with two nearly identical conformers in the asymmetric unit (molecules **3A** and **3B**). The aromatic and carbonyl groups in molecules **3A** and **3B** are substantially far from coplanarity with dihedral angles of 35.8° and 41.2°, respectively. A common feature in the crystal structures of **2** and **3** is that they pack in face-to-face centrosymmetric arrangements. The packing structure of benzosuberone **3** is also characterized by a close contact between the carbonyl group and the axial α-hydrogen of neighboring molecules A and B, which is indicated by a dashed line

(24) Migirdicyan, E.; Baudet, J. *J. Am. Chem. Soc.* **1975**, *97*, 7400−7404.
(25) Flynn, C. R.; Michl, J. *J. Am. Chem. Soc.* **1974**, *96*, 3280−3288.
(26) (a) Lutz, H.; Lindqvist, L. *Chem. Commun.* **1971**, 493−494. (b) Lutz, H.; Bréhéret, E.; Lindqvist, L. *J. Phys. Chem.* **1973**, 1758−1762.
(27) Khalaf, A. A.; Abdel-Wahab, A.-M.; El-Khawaga, A. M.; El-Zohry, M. F. *Bull. Soc. Chim. Fr.*, **1984**, 258−291.

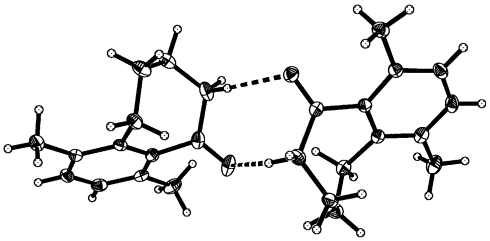

FIGURE 10. X-ray view of the C−H···O═C interaction between adjacent molecules in crystals of dimethylbenzosuberone (**3**).

TABLE 2. X-ray- and MM3-Determined Structural Parameters of Ketones 1a, 2, and 3

param	ideal value[a]	struct detmn	**1a**	**2**	**3A** (**3B**)
D (Å)	*b*	X-ray	n.a.	3.050	2.919 (3.016)
		MM3	2.730	3.004	3.113
Ω (deg)	*c*	X-ray	n.a.	2.0	35.8 (41.2)
		MM3	8.0	0	45.1
d (Å)	2.7	X-ray	n.a.	2.290	2.185 (2.311)
		MM3	1.86		
Δ (deg)	90−120	X-ray	n.a.	95.9	95.3 (91.8)
		MM3	108		
θ (deg)	180	X-ray	n.a.	135.5	130.6 (128.0)
		MM3	131.5		
ω (deg)	0	X-ray	n.a.	3.0	41.0 (45.3)
		MM3	8		

[a] The ideal values noted relate to the optimum ground-state geometries suggested by Scheffer in refs 34 and 35; please see text. [b] The ab initio calculated C···O distance in the transition state is ca. 2.54 Å (ref 36). [c] A dihedral angle Ω = 0° places the hydrogen donor and the carbonyl coplanar.

in Figure 10. With C−H···O═C distances of 2.417 and 2.791 Å, this interaction can be considered a hydrogen bond between the acidic α-hydrogen and the carbonyl oxygen. Although the close proximity between these two groups suggests the possibility of an intermolecular H-transfer reaction, we have not observed the formation of dimers, by hydrogen transfer and biradical collapse, or disproportionation products from an intermediate radical pair.

The molecular mechanics MM3 structure of **1a** has structural features between those of **2** and **3**. The cyclohexanone ring adopts a twist-boat conformation and the planes of the carbonyl and aromatic groups make a dihedral angle of 10°. The reliability of the calculated structure of **1a** was confirmed by comparing the molecular mechanics structures of **2** and **3** with those determined by X-ray diffraction. Several structural parameters determined by X-ray and force field calculations that are relevant to the hydrogen transfer reaction (vide infra) are listed in Table 2. Since the hydrogen positions in the X-ray and MM3 structures are not as reliable, the agreement between the MM3 and experimental structures in the case of **2** and **3** was judged by the excellent agreement of parameters involving heavy atoms such as the distance, *D*, between the methyl group and carbonyl oxygen, and the angle Ω, describing the dihedral angle between the planes of the aromatic and methyl groups and that of the carbonyl (Figure 11).

Structure−Reactivity Correlations. For H-atom transfer to occur at temperatures that are near absolute zero, the reaction must occur with minimum atomic and molecular motion. Orbital symmetry considerations suggest that an increase in overlap between the singly occupied n-orbital in the excited ketone and the σ^*-orbital of the transferring C−H bond will increase the rate of the reaction.[28−30] In fact, it is known that the rate of intramolecular H-transfer in solution is highly dependent on the conformational dynamics of the starting ketone and its ability to reach the transition state.[31,32] In rigid systems, Scheffer has proposed that a ground-state geometry can be used to estimate the likelihood and efficiency of the reaction.[33−35] He postulated that the ideal ground-state geometry should be as close as possible to the structure of the transition state.

Scheffer suggested that the best overlap between the active orbitals should be achieved from ground-state conformations where the O···H distance is within van der Waals contact, and having a H···O═C−C dihedral, *ω*, close to zero (Figure 11). The angle *ω* describes the position of the abstractable hydrogen relative to the plane containing the carbonyl and the nonbonding n-orbital. A collinear C−H··O arrangement and a C═O··H angle corresponding to an sp^2 (Δ = 120°) or sp (Δ = 90°) hybridization at the carbonyl oxygen are also expected to increase orbital overlap. Scheffer suggested that the "ideal" geometry for hydrogen abstraction would be given by the following: $d = 2.7$ Å, Δ = 90−120°, $\theta = 180°$, and $\omega = 0°$.

Ab initio calculations of the transition state of butanal in the Norrish Type II reaction by Dorigo and Houk[36] and of pentan-2-one by Chandra and Sreedhara Rao[37] indicate that the geometry of the transition state is congruent with the ground-state geometry suggested by Scheffer. The C═O···H angle, Δ = 105°, is within Scheffer's ideal of 90−120°. Although the C−H···O alignment is nonlinear, with $\theta = 153°$, a value of $\theta = 180°$ would be difficult to achieve in a cyclic six-membered transition state. A forming O−H bond distance of 1.19 Å and a breaking C−H bond distance of 1.35 Å would not be possible in a ground-state structure, but the former is within the range of $d = 2.7$ Å proposed by Scheffer. Although the ab initio calculations of aliphatic carbonyls predict a pyramidal triplet, experimental and computational evidence indicates that aromatic ketones remain planar.

From the three aryl ketones considered in this study, compound **1a** has structural parameters that approach

(28) Michl, J.; Bonacic-Koutecky, V. *Electronic Aspects of Organic Photochemistry*; Wiley-Interscience: New York, 1990.
(29) Salem, L. *Science* **1976**, *191*, 822−30.
(30) Dauben, W. G.; Salem, L.; Turro, N. J. *Acc. Chem. Res.* **1975**, *8*, 41−54
(31) Wagner, P. J. *Acc. Chem. Res.* **1983**, *16*, 461−467.
(32) Lewis, F. D.; Johnson, R. W.; Johnson, D. E. *J. Am. Chem. Soc.* **1974**, *96*, 6090−6099.
(33) Gudmundsdottir, A. D.; Lewis, T. J.; Randall, L. H.; Scheffer, J. R.; Rettig, S. J.; Trotter, J.; Wu, C.-H. *J. Am. Chem. Soc.* **1996**, *118*, 6167−6184.
(34) Scheffer, J. R.; Dzakpasu, A. *J. Am. Chem. Soc.* **1978**, *100*, 2163−73.
(35) (a) Scheffer, J. R.; Garcia-Garibay, M. A.; Nalamasu, O. *Org. Photochem.* **1987**, *8*, 249−347. (b) Scheffer, J. R. *Solid State Organic Chemistry*; Desiraju, G. R., Ed.; VCH: Amsterdam, The Netherlands, 1987; pp 1−45.
(36) (a) Dorigo, A. E.; McCarrick, M. A.; Loncharich, R. J.; Houk, K. N. *J. Am. Chem. Soc.* **1990**, *112*, 7508−7514. (b) Dorigo, A. N.; Houk, K. N. *J. Am. Chem. Soc.* **1987**, *109*, 2195−2197.
(37) (a) Sreedhara Rao, V.; Chandra, A. K. *Chem. Phys.* **1997**, *214*, 103−112. (b) Chandra, A. K.; Sreedhara Rao, V. *Chem. Phys. Lett.* **1998**, *270*, 87−92

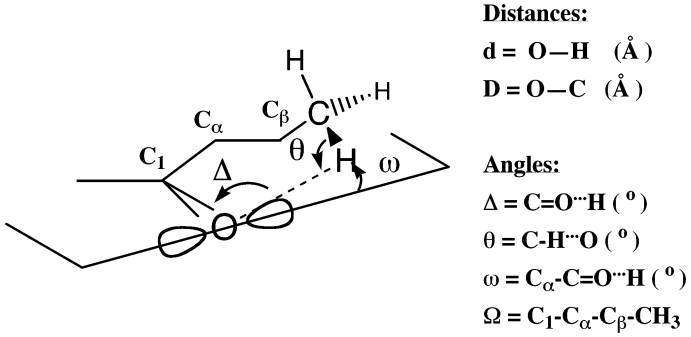

FIGURE 11. Geometric parameters that describe the geometric relation between the abstractable hydrogen and the target oxygen carbonyl.

Scheffer's ideal reaction geometry more closely (Table 2 and Figure 9). The distance between the carbonyl oxygen and transferring hydrogen is shortest (d = 1.86 Å), and the angles $\Delta = 108°$ and $\omega = 8°$ are close to the proposed ideal of 90−120° and 0°, respectively. The abstractable hydrogen is close to the carbonyl oxygen and close to the plane of the singly occupied n-orbital. Accordingly, with tunneling rates of $k_D = 10^3\ s^{-1}$ and $k_H \approx 10^6$ for deuterium[6,7] and hydrogen,[7] dimethyltetralone (**1a**) is the most reactive aryl ketone of the three.

On the other extreme of the tunneling reactivity is dimethylindanone (**2**), which appears to be completely photostable. However, on the basis of structural parameters alone, one might have expected compound **2** to be the second most reactive. The most significant difference between the MM3 structure of **1a** and the X-ray structure of **2** is the longer distances, d and D, between hydrogen and oxygen, and carbon and oxygen. However, with a value of d = 2.29 Å, compound **2** is well within the ideal limit of d = 2.7 Å suggested by Scheffer. We suggest that the difference in reactivity between **1a** and **2** may be due to their different electronic configurations. While compound **1a** is mainly an n,π* triplet with a ketone-centered excitation, dimethylindanone (**2**) has a greater contribution from a π,π* state and has more aromatic character. Differences in H-transfer rates between ketones with different electronic states have been well-documented. The lack of reactivity from indanone **2** may also reflect the high sensitivity of quantum mechanical tunneling to the height and width of the barrier. The five-membered ring of compound **2** pulls the carbonyl oxygen away from the *o*-methyl, increasing the C═O···H−C distance. When the O···H distance, d, is larger, the C−H bond must be stretched further to reach the transition state, effectively increasing the height and width of the barrier.

The lack of tunneling in **2** may also indicate that the rigid indanone structure does not possess reaction-promoting degrees of freedom such as those previously postulated for compound **3**. With zero-point-energy tunneling rates of 70−100 s^{-1} and a chromophore that has a relatively long excited-state lifetime (30 ms in the case of **6**), the tunneling reactivity of **3** may be attenuated with respect of that of **1a** by a combination of structural and electronic effects. It is interesting to note that the ground-state geometries of the two conformations of **3** (**3A** and **3B**) cover a range that includes the structural parameters determined for compound **2**. For instance, nonbonded O···H−C distances for **3A** (d = 2.185 Å) and **3B** (d = 2.311 Å) are shorter and longer, respectively, than those of dimethylindanone (**2**) (d = 2.29 Å). The most striking differences between the structures of **3A** and **3B** as compared to those of **1a** and **2** are the values of the angle ω. Unlike the structures of **1a** and **2**, hydrogens on the *o*-methyl group of **3** are relatively far from the plane of the active n-orbital. With values of $\omega = 41.0°$ and 45.3°, the structure of **3** must undergo skeletal motion to bring the transferring hydrogen close to the active n-orbital.

SCHEME 4

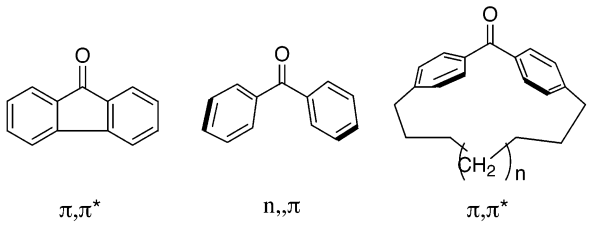

While qualitative relations may be suggested with regard to the role of the ground-state reaction geometry on the tunneling efficiency, the effects of structure on the electronic properties of the excited state are rather puzzling. The excited states of compounds **1a**, **2**, and **3** can be described has hybrid states with different amounts of n,π* and π,π* character. Our analysis of the vibrational resolution and triplet lifetimes indicates that the contribution from the reactive n,π* state is highest for the tetralones, it decreases in the case of the dibenzosuberones, and it has a minimum in the five-membered-ring indanones. Considering that all three compounds have the same alkyl group substitution around the aromatic ketone chromophore, one may conclude that differences in excited-state configuration must arise from changes in conjugation between the aromatic ring and ketone. The dihedral angles between their corresponding planes vary from 8° (MM3) in the case of **1a** to 3° in the case of **2**, with a maximum of 35.8° and 41.2° in the case of **3A** and **3B**. A dependence of the excited state electronic configuration with the conjugation angle between the ketone carbonyl and the aromatic ring had been previously observed in diaryl ketones (Scheme 4). While fluorenone has a predominant π,π* character, benzophenone is a typical n,π* ketone. It is also known that an increase in the twist angle between the carbonyl and aryl groups in a series of macrocyclic benzophenone derivatives decreases the contribution from the n,π* state. One may conclude that fully conjugated aryl ketones possess an aromatic π,π* state, a small twist angle appears to favor

a ketone-centered n,π^* state, and surprisingly, large twist angles appear to favor a triplet state with more π,π^* character.

Conclusions

We have shown that hydrogen transfer by quantum mechanical tunneling in *o*-methyl aryl ketones is extremely sensitive to the electronic configuration of the excited state and to the reaction geometry. On the basis of phosphorescence spectra and triplet lifetime measurements, the triplet state of *o*-methyl indanone **2** can be described in terms of a predominant π,π^* electronic configuration. As far as we can tell, indanone **2** is completely photostable under cryogenic conditions. With a seven-membered ring, *o*-methylbenzosuberone (**3**) has less π,π^* character than dimethylindanone (**2**) but significantly more than the six-membered ring dimethyltetralone (**1a**). Compound **3** reacts at all temperatures analyzed. The reaction below 50 K occurs exclusively by quantum mechanical tunneling along the zero-point-energy surface. An unusually small and temperature-invariant isotope effect was interpreted in terms of a vibrationally assisted quantum mechanical tunneling process. A close analysis at the structures of compounds **1a**, **2**, and **3** reveals relatively small differences, which highlights the great structural sensitivity of quantum mechanical tunneling reactions.

Acknowledgment. Financial support by the National Science Foundation (through grant CHE0073431) is gratefully acknowledged.

Supporting Information Available: X-ray molecular structures, packing diagrams, and data tables for compounds **2** and **3**. This material is available free of charge via the Internet at http://pubs.acs.org.

JO016210R